Current sink and source patterns in the prefrontal cortex of a behaving monkey

Kazuhiro Sakamoto[a] Norihiko Kawaguchi[b], Kohei Yagi[b], Yoshia Matsuzaka[b], Norihiro Katayama[c], Tetsu Tanaka[d] and Hajime Mushiake[b,e]

[a]Research Institute of Electrical Communication, Tohoku University
2–1–1 Katahira, Aoba-ku, Sendai 980–8577, Japan
[b]Department of Physiology, Tohoku University School of Medicine
2–1 Seiryo-cho, Aoba-ku, Sendai 980–8575, Japan
[c]Graduate School of Information Sciences, Tohoku University
01 Aza Aoba, Aramaki, Aoba-ku, Sendai 980-8579, Japan
[d]Graduate School of Biomedical Engineering, Tohoku University
01 Aza Aoba, Aramaki, Aoba-ku, Sendai 980-8579, Japan
[e]The Core Research for Evolutional Science and Technology Program (CREST), JST
Goban-cho, Chiyoda-ku, Tokyo, 102–0076, Japan
Email: sakamoto@riec.tohoku.ac.jp, kawaguchi@med.tohoku.ac.jp, b1mb1114@st.med.tohoku.ac.jp, matsuzay@med.tohoku.ac.jp, katayama@ecei.tohoku.ac.jp, ttanaka@lbc.mech.tohoku.ac.jp, hmushiak@med.tohoku.ac.jp

Abstract– Investigation of the input–output structures of cortical circuits is necessary to clarify their dynamical properties. However, conventional physiological studies have focused primarily on spiking activity, which reflects the output of neurons or neuronal circuits. Recently developed multicontact electrodes enable the evaluation of synaptic inputs through current source density (CSD) analysis of local field potentials (LFPs) in addition to recording spikes. Here, we present preliminary findings of CSD patterns in the prefrontal cortex (PFC) of a behaving monkey and provide examples of how PFC neurons change their firing properties dynamically depending on input to PFC local circuits.

1. Introduction

One of the fundamental missions of neuroscience is to assess the input and output of neuronal circuits to elucidate their functional properties. It is particularly important to uncover the executive functions associated with the prefrontal cortex (PFC) [1] because recent studies have shown that the output properties of PFC neurons dynamically change depending on their inputs [2–4]. However, most conventional electrophysiological studies using microelectrodes have investigated spike activity, which reflects the output of, rather than input to, neurons or neuronal circuits.

Recently developed multicontact electrodes enabled us to record neural activity from regularly spaced recording sites [5–7]. Furthermore, we are able to estimate the current source density (CSD) of synaptic input to local circuits by calculating the second-order spatial difference of local field potentials (LFPs) [8].

Here, we present the preliminary results of a CSD analysis applied to spatiotemporal patterns from the PFC of a behaving monkey together with simultaneously recorded spike activity.

2. Methods

2.1. Subjects

Experiments were performed on one male monkey (*Macaca fuscata*; 9.0 kg). All experimental protocols were approved by the Animal Care and Use Committee of Tohoku University. Furthermore, all animal protocols conformed with the National Institutes of Health (NIH) Guidelines for the Care and Use of Laboratory Animals.

2.2. Behavioral Task

The monkey was trained to perform a shape manipulation task (Fig.1) that required step-by-step movements using manipulanda. The goal was to fit the test shape to the sample shape. In each trial, a single shape was randomly selected from a set of display shapes.

After a fixation spot appeared on the screen, a sample shape was displayed for 1 ± 0.2 s (sample cue). Following a 1 ± 0.2-s delay period (delay), a test shape that was homothetic to the sample shape but transformed (i.e., expanded/contracted and rotated) was displayed for 1 ± 0.2 s (test cue). Thereafter, the color of the fixation point

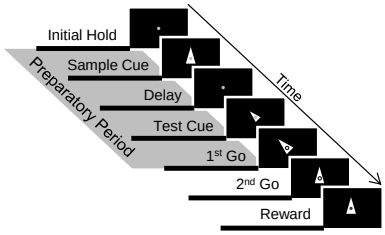

Figure 1 Temporal sequence of events in the shape manipulation task.

was changed, which served as a go signal to initiate the first-step movement (first go). The animal was required to execute a movement within a specific time window and to wait until the second go signal (second go) appeared. At each go signal, the animal was allowed to make a single, one-handed movement. He was also permitted to perform any number of steps as long as a movement was executed within the time window. When the test shape was successfully transformed to fit the sample shape, the animal was rewarded with an isotonic drink.

Shape manipulation was linked to the movements of two manipulanda installed in the chair that were operated with the right or left wrist. Left-hand supination and pronation controlled expansion (double the area) and contraction (half the area), respectively, and right-hand supination and pronation controlled rightward rotation (-45 deg.) and leftward rotation (45 deg.) of the test shape, respectively.

To dissociate the movements of the arms and the cursor, we trained the monkey to perform the task with two different arm-cursor assignments. In the first cursor assignment, left-hand supination, left-hand pronation, right-hand supination, and right-hand pronation were assigned to expansion, contraction, rightward rotation, and leftward rotation, respectively. In the second assignment, left-hand supination, left-hand pronation, right-hand supination, and right-hand pronation were assigned to leftward rotation, rightward rotation, contraction, and expansion, respectively. The assignment was changed every 68 trials. In the first half of the 68-trial block, the contour of the sample cue was displayed during the test cue period (visually guided task), and the contour was not displayed in the latter half (memory-guided task). The success rate was 89% [9].

2.3. Electrophysiological Recording

The surgical procedure has been described previously [3]. Following surgery, the cortical sulci were identified using a magnetic resonance imaging (MRI) scanner (OPART 3D-System; Toshiba, Tokyo, Japan) and by mapping single-unit activity recorded using conventional metal electrodes.

Electrophysiological recordings were performed using linear-array multi-contact electrodes (U-Probe; Plexon, Inc., Dallas, TX, USA) containing 15 recording contacts (impedance, 0.3–1.3 MΩ at 1 kHz) with an inter-contact spacing of 200 μm. We used a guide needle to introduce the electrode. Once the electrode reached the dura mater, advancement of the guide needle was stopped, and the electrode was inserted into the cortex perpendicular to its surface. The electrode was precisely positioned. It was lowered until the multi-unit activity initially encountered through the bottommost contact (ch. 15) was detected through the top contact (ch. 1). Signals from the electrode were collected using a data-acquisition system (Neuralynx, Bozeman, MT, USA). LFP and spikes were obtained by band-pass filtering the raw signal from 0.1 Hz to 475 Hz and from 600 Hz to 6 kHz, respectively.

2.4. Data Analysis

Only the data obtained from correct trials with a minimum of two steps were included in the analyses. LFP signals were averaged across trials. CSD was calculated from the LFPs using numerical differentiation to approximate the second-order spatial derivative of the voltage recorded at each recording contact [8]. CSD at the *n*th contact, D_n, at a time point was calculated as follows:

$$D_n = -\sigma\,[\varphi\,(n+1) + \varphi\,(n-1) - 2\,\varphi\,(n)] / \Delta^2, \qquad (1)$$

where σ is tissue conductivity assumed to be constant (0.3 S/m), φ (n) is the LFP signal at the *n*th contact of the electrode, and Δ is the spacing between the neighboring electrode contacts (200 μm). Negative and positive D_n values indicate the current sink and current source at the *n*th contact, respectively. CSD waveforms were smoothed

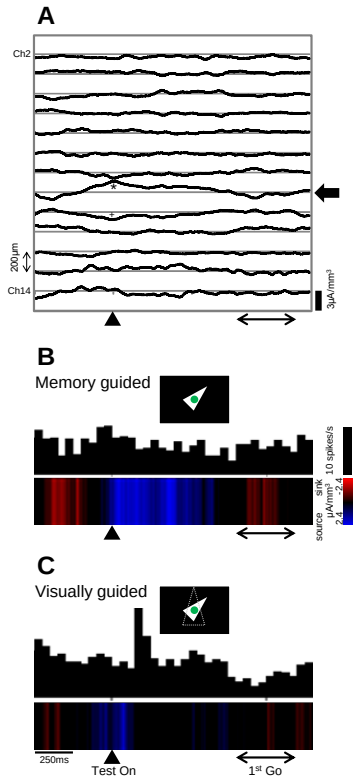

Figure 2. Example of a task-dependent current source pattern. **A**. Trial-average CSD pattern at one recording site (23.0, 33.0) at the mediolateral (ML) and anteroposterior (AP) coordinates. Asterisks denote significant and valid current sinks or sources. Crosses denote significant but invalid sinks or sources (see text). **B**. CSD and spike patterns recorded from ch.10 (arrow in **A**) simultaneously with execution of the memory guided task. **C**. CSD and spike patterns recorded from ch. 10 simultaneously with execution of the visually guided task.

using a sliding averaging window of 50 ms. The presence of a peak and trough, namely the current source and sink, respectively, was statistically tested using a bootstrapping method. We defined the reference period as the time from -1,000 to -500 ms relative to the sample cue onset for each dataset because no salient current sinks or sources were observed in any dataset during this period. We calculated all possible quasi-CSD values by shuffling the channel number of the electrode at each time point, then we obtained lower and upper significance levels of $P = 0.05$ and $P = 0.95$, respectively. Only epochs exhibiting significant sinks or sources in consecutive time steps for more than 50 ms were regarded as significant. When significant sinks and sources were detected simultaneously from adjacent contacts, we selected the one that exhibited the larger magnitude and deemed it valid so as to exclude return or artifactual current density.

3. Results

We recorded LFP signals from 10 sites on the ventral side of the PFC principal sulcus. Each dataset included approximately 140 correct trials with a minimum of two steps (i.e., entire task variation). Meanwhile, we recorded from stable neurons. Data were analyzed for the preparatory period of the task.

Figure 2A is an example of a trial-average CSD pattern recorded from the inferior convexity of the ventral PFC. In this pattern, a significant current source was observed in ch. 10 at approximately the onset of the test cue. At the same time, we observed a significant current sink in the adjacent channel below, namely ch. 11. However, the sink was not considered valid because the magnitude was lower than that of the source in ch. 10.

A comparison of the CSD pattern and simultaneous single-unit activity recorded at ch. 10 for the memory- and visually guided tasks are shown in Figure 2 B and C, respectively. In the memory-guided task, the strong current source emerged close to the onset of the test cue, and the firing rate of the simultaneously recorded single unit was virtually flat during this period (Fig. 2B). In contrast, we observed a transient increase in the firing rate of the single unit immediately following termination of the current source, whose duration was quite short in the visually guided task (Fig. 2C). These findings illustrate that the current source is not always a passive return current but may reflect inhibitory synaptic input. That is, the strong current source inhibited an increase in firing rate in this case.

The task-dependent changes in the significant and valid sink and source currents for all recording sites are shown in Figure 3. The 10 recording sites can be divided into convex (six sites) and sulcus (four sites) groups [10] as indicated by the dashed lines in Figure 3. In the convex group, the electrodes penetrated the cortex vertically, whereas the electrodes were inserted horizontally into the ventral bank of the principal sulcus in the sulcus group. As a result, few significant and valid sinks and sources were observed in the upper contacts (ch. 2–8) of the convex group compared with the sulcus group ($P < 0.05$, binominal test). We compared the task-dependent current sink and source patterns between the two groups.

Significant and valid sinks were observed only in the sulcus group during the sample cue period and were dominant in that group during the test cue period ($P < 0.05$, binominal test for both). Furthermore, significant and valid sources were dominant in the sulcus group during the peri-sample onset ($P < 0.05$, binominal test) and delay ($P < 0.05$, binominal test) periods. The absence of significant and valid sink currents during the sample cue period in the convex group was statistically significant ($P < 0.05$, binominal test); however, we observed a considerable number of significant and valid source currents during the test cue period ($P < 0.05$, binominal test).

4. Discussion

We simultaneously recorded multiple LFPs and spike signals from the PFC of a behaving monkey. A CSD analysis revealed task-dependent current sink and source patterns.

Current source is often considered a passive return current accompanied by an excitatory synaptic stimulation [11]. However, we observed several current sources that had magnitudes larger than those of the adjacent sinks and that appeared to be biologically meaningful; specifically, they appeared to reflect inhibitory synaptic input. This view is supported by our finding of consistent spike activity at the same contact where a significant and valid current source was observed. Current source as a reflection of inhibitory synaptic input has been reported previously [12]. Future studies are needed to establish a more accurate method for defining current source that exclude simply describing it as passive return current.

We were able to distinguish between CSD signals in the inferior convex and the principal sulcus. In the convex group, significant and valid current sinks and sources were virtually absent at the upper contacts (ch. 2–8). In the sulcus group, significant sinks were observed frequently at lower and upper contacts. These differences presumably reflect the different orientation of the electrodes in the convex and sulcus groups.

The sulcus group exhibited several current sinks during the sample and test cue periods, but not during the delay period, a time period when numerous sinks were observed in the convex group. These differences likely reflect anatomical or functional heterogeneity in our recording sites [1].

Our physiological technique coupled with the application of multicontact electrodes and CSD analysis, enabled the examination of fine cortical input structures. Thus, combined analysis of the spike activities reflecting neuronal output can reveal the functional roles of cortical circuits in greater detail.

Acknowledgments

This research was supported by a Grant-in-Aid for Scientific Research (C) (#22500283, #26350991) by the Japan Society for the Promotion of Science; a Grant-in-Aid for Scientific Research on Innovative Areas "The study on the neural dynamics for understanding communication in terms of complex hetero systems (number 4103)" (#22120504, #24120703), "Elucidation of the neural computation for prediction and decision making (number 4303)" (#26120703) and "Comprehensive Brain Science Network" of the Ministry of Education, Culture, Sports, Science, and Technology of Japan; Creative Interdisciplinary Research Program in Frontier Research Institute for Interdisciplinary Sciences of Tohoku Univ.; the Japan Science and Technology Agency (CREST).

References

[1] R. E. Passingham and S. P. Wise, The neurobiology of the prefrontal cortex, Oxford, 2012.
[2] Y. Katori, K. Sakamoto, N. Saito, J. Tanji, H. Mushiake, and K. Aihara, "Representational switching by dynamical reorganization of attractor structure in a network model of the prefrontal cortex," *PLoS Comput. Biol.*, vol.7, e1002266, 2011.
[3] K. Sakamoto, H. Mushiake, N. Saito, K. Aihara, M. Yano and J. Tanji, "Discharge synchrony during the transition of behavioral goal representations encoded by discharge rates of prefrontal neurons," *Cereb. Cortex*, vol.18, pp.2036–2045, 2008.
[4] K. Sakamoto, Y. Katori, N. Saito, S. Yoshida, K. Aihara, and H. Mushiake, "Increased firing irregularity as an emergent property of neural-state transition in monkey prefrontal cortex," *PlosONE*, vol.8, e80906, 2013.
[5] K. D. Wise, and K. Najafi, "Microfabrication techniques for integrated sensors and microsystems," *Science*, vol. 254, pp.1335-1342, 1991.
[6] T. Jellema and J. A. W. M. Weijnen, "A slim needle-shaped multiwire microelectrode for intracerebral recording," *J. Neurosci. Methods*, vol.40, pp.203-209, 1991.
[7] R. Kobayashi, S. Kanno, S. Lee, T. Fukushima, K. Sakamoto, Y. Matsuzaka, N. Katayama, H. Mushiake, M. Koyanagi, and T. Tanaka, "Development of double-sided Si neural probe with microfluidic channels using wafer direct bonding technique," *IEEE EMBS*, vol.4, pp.96-99, 2009.
[8] C. Nicholson and J. A. Freeman, "Theory of current source density analysis and determination of conductivity tensor for anuran cerebellum," *J. Neurophysiol.*, vol.38, pp.356-368, 1975.
[9] K. Sakamoto, N. Kawaguchi and H. Mushaike, "Is advance planning of sequential movements reflected in the behavior of monkeys?" *Ann. Jpn Neural Netw. Soc.*, vol.22, 3-19, 2012.
[10] K. Sakamoto, N. Kawaguchi, K. Yagi and H. Mushiake, "Spatiotemporal patterns of current source density in the prefrontal cortex of a behaving monkey," *Neural Netw.*, (in submission).
[11] G. T. Einevoll, C. Kayser, N. K. Logothetis, and S. Panzeri, "Modelling and analysis of local field potentials for studying the function of cortical circuits," *Nat. Rev. Neurosci.*, vol.14, pp.770-785, 2013.
[12] N. A. Lambert, A. M. Borroni, L. M. Grover and T. J. Teyler, "Hyperpolarizing and depolarizing $GABA_A$ receptor-mediated dendritic inhibition in area GA1 of the rat hippocampus," *J. Neurophysiol.*, vol.66, pp.1538-1548, 1991.

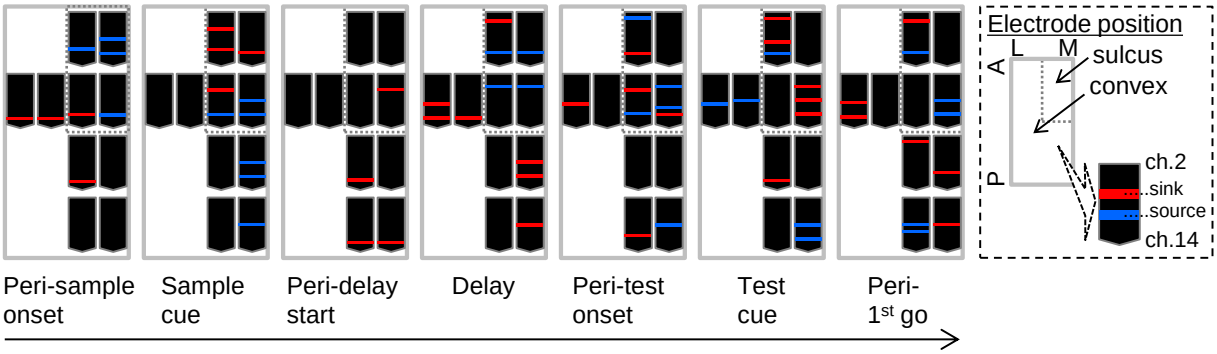

Figure 3 The spatiotemporal patterns of significant sink and source currents. The position of each pentagonal shape represents the position of a recording site in the ventral prefrontal cortex. The vertical placement of the red and blue bars within the pentagon represent the vertical positions of significant and valid sink and source currents, respectively. The dotted lines show the border between the convex and ventral bank of the principal sulcus. Peri-sample onset (-400 to 100 ms), sample cue (100 to 600 ms), peri-delay start (600 to 1,100 ms), and delay (1,100 to 1,600 ms) of sample cue onset. Peri-test onset (-400 to 100 ms), test cue (100 to 600 ms), and peri-1st go (600 to 1,100 ms) of the test cue onset. Inset: A, anterior; P, posterior; M, medial; and L, lateral.